

## **Chapter - 5**

# **Geochemistry of Quaternary Alluvium in the Luni River Basin**

## 5.1 Introduction

Weathering and subsequent sedimentary processes play a major role in sculpting Earth's surface and redistributing the eroded material from source rocks to depositional sinks. Globally, rivers are the main transporting agents of these eroded sediments (Martin and Whitfield, 1983). Thus, the geochemistry of river borne clastic sediments provides important insights into the source rock characteristics. However, the geochemical behaviour of sediments also depends on the extent of chemical weathering, physical sorting during transportation and diagenetic alterations. Therefore, the geochemical provenance study of sediments can also be utilized to understand weathering in the source region (Singh and Rajamani, 2001). Trace elements, especially the Rare Earth Elements (REE), are considered useful for understanding these processes (Taylor and McLennan, 1985). In many instances, however, the REE can also be redistributed within a weathering profile without a net loss or gain (Condie, 1991; Duddy, 1980; Nesbitt, 1979; Sharma and Rajamani, 2000) and as a consequence, different sediment loads (suspended and bed loads) may show different REE abundances/patterns in comparison to their source rocks. It has been observed that REE fractionations are more prominent when physical weathering dominates over chemical weathering (Viers et al., 2009), whereas intense chemical weathering obliterates any such discrepancy between the source and the product. Predominance of chemical weathering over physical weathering, however, requires appropriate climatic conditions in the catchment. Therefore, provenance studies need to evaluate the weathering conditions in the source regions carefully before interpreting the geochemical data of clastic sediments.

Present study deals with the fluvial deposits of the Luni River originating from a Pre-Cambrian terrain and flows along the southern margin of the Thar desert (Fig. 5.1). Generally, arid zone rivers respond quickly to minor perturbations in climate and the Luni River is not an exception (Kar et al., 2001). The river originates from the Proterozoic Delhi-Aravalli fold belt in the east and flows through a granitic-rhyolitic catchment. However, the contributions of these lithologies to the sediment budget is not well constrained. The dominance of physical weathering over chemical weathering in this region makes the problem more interesting. In the present work we have studied trace element geochemistry and Sr -Nd isotopic ratios of sediments deposited in the Luni basin during the Quaternary period. The elemental geochemistry of different fluvial deposits has been studied to

understand the changing effect of weathering on different source rocks and sediment produced by it. Using the Sr-Nd isotopic ratio of the sediments the contributions from different source rocks have been quantified.

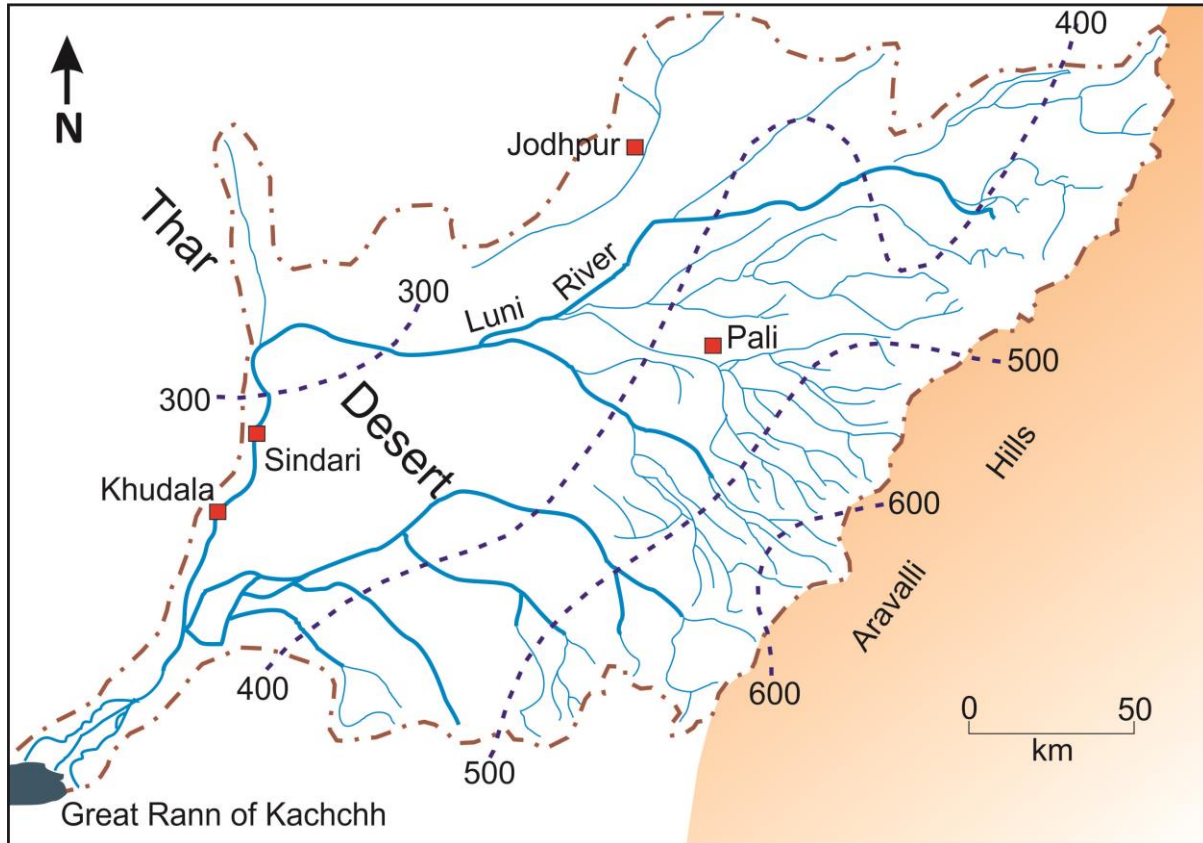


Figure 5.1: The drainage system of the Luni river basin and the isohyets are representing the average rainfall of the basin.

## 5.2 Alluvial stratigraphy, the catchment and the study area of the Luni basin

The Luni river system is the major drainage of the Thar Desert and flows in the south-east corner of the desert. The river originates in the Aravalli range and flows westward draining into the Great Rann of Kachchh (Fig.5.1). The upper catchment of the river generally receives 500-600 mm/yr of rainfall (Fig. 5.1). However, most of its drainage lies within the semi-arid region with annual rainfall of 300-400 mm, a large amount of which is received during the SW Indian Monsoon. Rest of the year, the discharge is almost absent and

aeolian sands accumulate in the river channel. In monsoonal floodings the aeolian sands get washed out and re-deposited downstream. The Luni possesses all the traits of an ephemeral river.

### 5.2.1 Stratigraphy of the Luni Alluvium

The general stratigraphy and facies architecture of the Luni alluvium have been worked out by many earlier workers (Jain et al., 2005; Kale et al., 2000; Kar et al., 2001; Sharma et al., 1984). Figure 5.2 presents a general stratigraphy of the Luni alluvium (Jain et al., 2005). The facies architecture of the Luni alluvium is described below.

- There are two distinct types of sedimentary sequences in the Luni basin.
- The older Type-1 sequence was deposited probably during the Pliocene (ages beyond luminescence dating, thus the minimum age is considered 200 ka).
- Type -1 sequences consist of fining upward sequences of alternate gravelly beds and mud-dominated horizons. These facies mainly represent deposition in a braided river system. Absence of aeolian sand horizons indicate a much wetter depositional condition, probably before the formation of the dune fields in this region.
- There exist a long hiatus after the deposition of Type- 1 sequence.
- Type – 2 sequences were deposited during the Pleistocene to Holocene periods over the last 100 ka.
- The facies architecture of Type-2 sequence is quite different from the older deposits. The successions in it suggest a change in the depositional environment. They represent deposition in fluctuating fluvio-aeolian environment. Three incision events with ages of 14ka, 9-11 ka and 3-1 ka have been identified with periods of increased rainfall.
- Unlike, the older deposits these horizons are dominated with sand.
- The deposition started with a gravelly bed followed by aeolian sand sheet and sheet wash deposits.
- The following period witnessed an increase in monsoonal precipitation during the beginning of the Holocene. As a consequence, several fining upward fluvial sand-silt units were deposited during the higher fluvial activities.
- Finally, the alluvial deposits were covered by aeolian sands reworked from older fluvial deposits. In the recent times slack water deposits get generated due to seasonal floods.

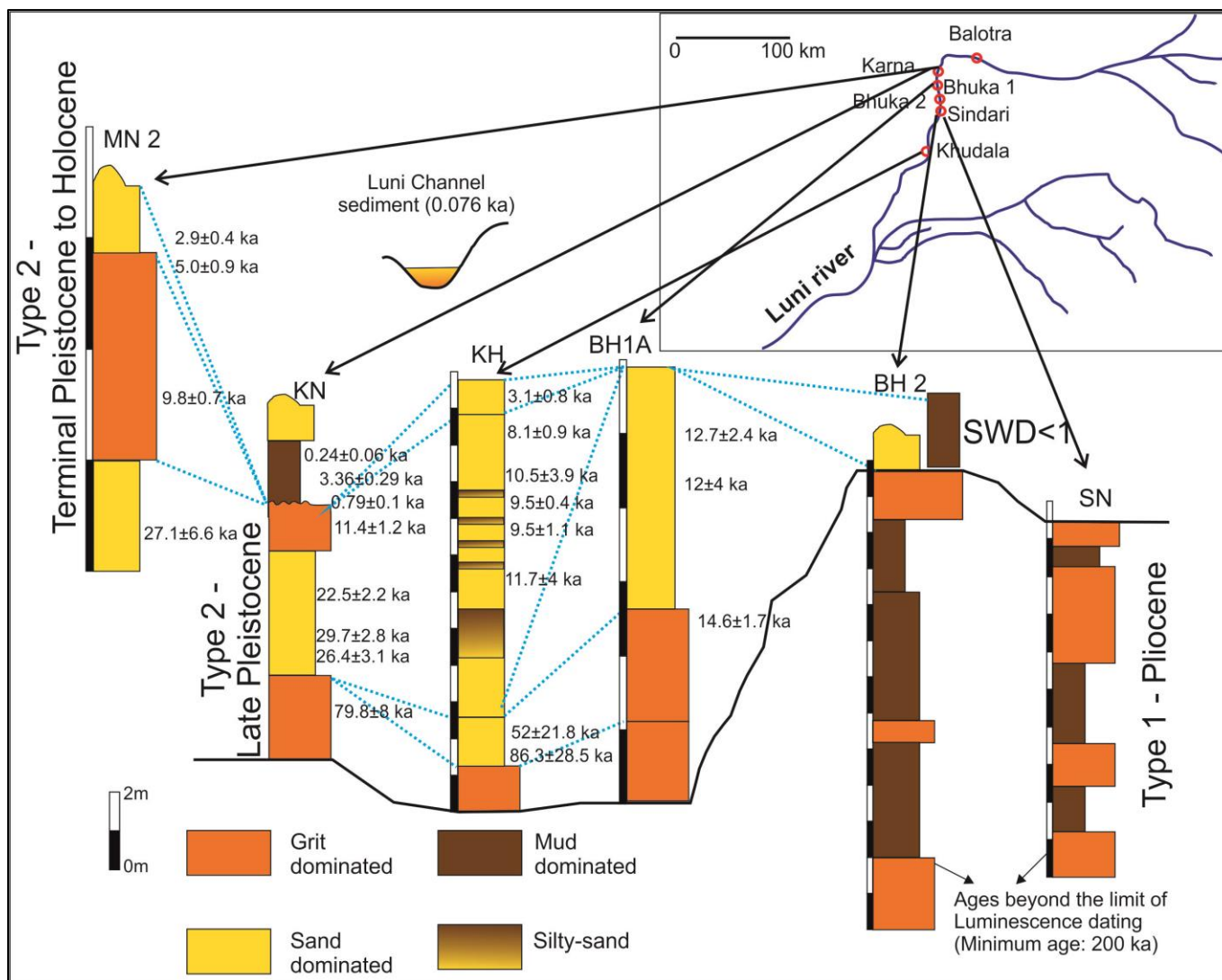


Figure 5.2: The stratigraphic framework of the Luni alluvium (modified after Jain et al., 2005).

- In the piedmont regions of the river and on the river bed, locally derived modern gritty-sand deposits can be observed.

### 5.2.2 Catchment of the Luni river

Figure 5.3 represents the catchment lithology of the Luni river basin. Based on the existing information the following observations can be made about this river system and its catchment.

- The river originates from the piedmont region of the major axial section of the Aravalli range where its elevation is highest (~1200m, between Ajmer and Mt. Abu).
- The rocks exposed along the upper catchment (the Aravalli ridges flanking the piedmont) of the river are mainly composed of schists, slates, gneisses and calc-silicates of Delhi Supergroup.
- Along with the metasedimentary rocks of the Delhi Supergroup, a suit of metamorphosed mafic-ultramafic rocks are exposed along the western margin of the Aravalli ranges (Volpe and Macdougall, 1990). They are representative of the suture zone between the Aravalli and the Delhi Supergroups (the type section is the Phulad Ophiolite). These rocks are exposed all along the catchment of the Luni (from Ajmer to Desuri) and its tributaries. They are mainly composed of massive amphibolites, hornblendites, meta-gabbros, serpentinites and dioritic dykes.
- Pockets of pre-Aravalli Banded Gneissic Complex (BGC) rocks are also exposed at the western margin of the mountain ranges.
- Syn to Post orogenic granites (e.g., Erinpura Granite) are exposed in the western part of the Aravalli ranges. At places exposures of the Malani rhyolites can also be found.
- Minor exposures of sedimentary rocks belonging to the Marwar Supergroup can be observed at the lower catchment of the Luni.
- In the downstream, most of the catchment is covered with old alluvium deposits and sand dunes.

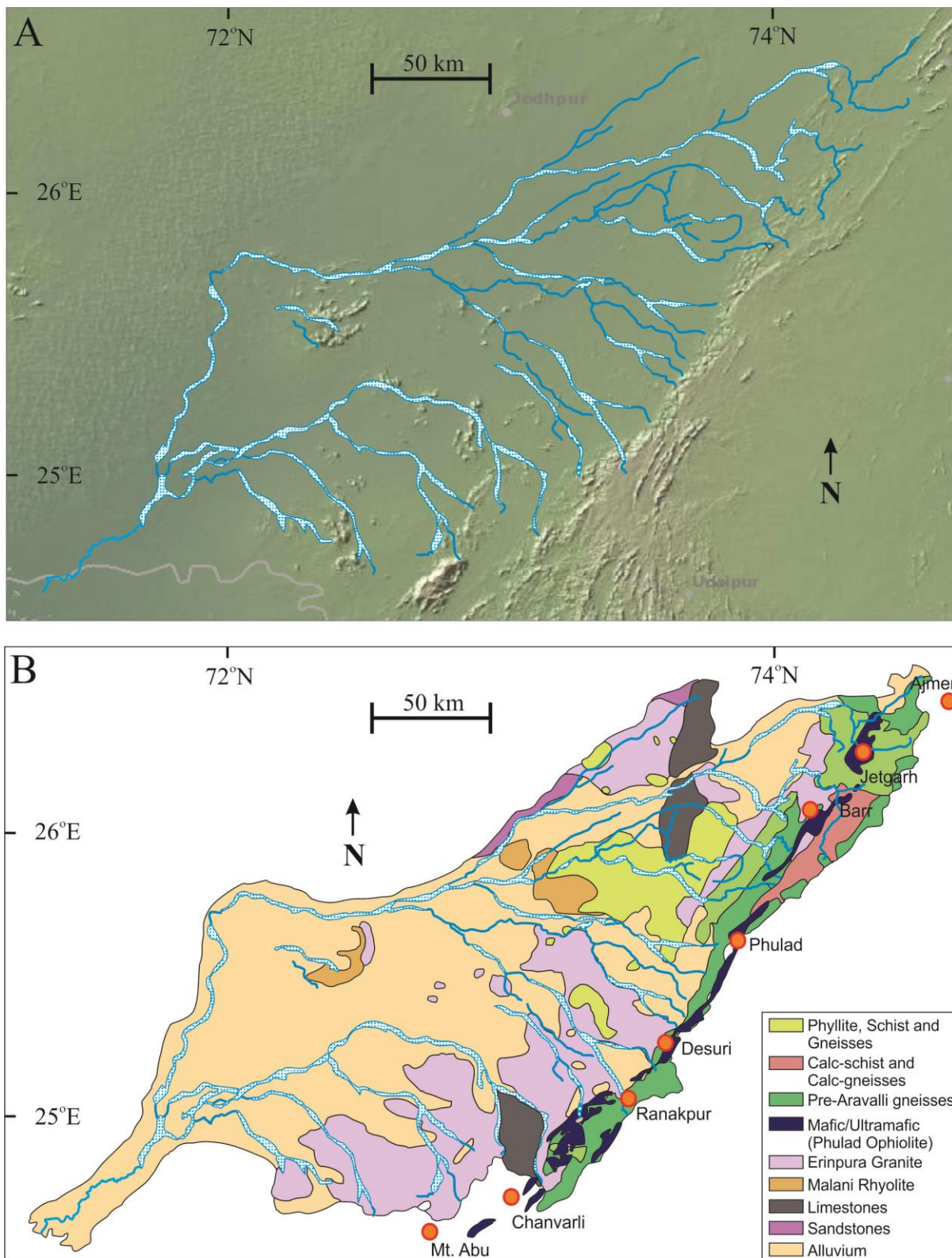


Figure 5.3: (A) Topographic map of the Luni river basin (National Centers For Environmental Information) showing the major elevated regions in the catchment. It can be observed that the river emerges from the piedmont region of the major axial heights of the Aravalli ranges.

(B) The lithological map of the catchment of the Luni river (modified from Sharma et al., 1984; Volpe and Macdougall, 1990).

### 5.2.3 The Study Area

Description of sample locations and samples used in the present study are presented below.

- Sampling for the Type-1 successions was done in the Sindari – Karna sector. The gritty-sand sediment horizons are heavily altered to clay and show compaction. A few unaltered gritty-sand deposits were found and sampled. We also sampled the silt-clay dominated horizons.
- The Type-2 successions were sampled at the Khudala section. At Khudala, samples were collected in regular intervals in a vertical profile. Sampling was done mainly from the fining upward sequences, from which alternate sand and silty-clay bands were sampled.
- Modern bed-load sediment comprising of gritty-sand were collected from the Dhal river bed (a tributary of the Luni) near the piedmont region where the river comes out of the Aravalli ranges. In addition, modern bedload sediment comprising mainly of gritty-sand was collected from the Karna region, further downstream of the river where it passes through very different lithologies.
- Modern deposits of suspended sediment were collected from the river banks.

## 5.3 Results and discussion

### 5.3.1 Trace element geochemistry

The trace element concentration and Sr-Nd isotopic compositions of the Luni river sediments are presented in table 5.1. The chondrite normalised and PAAS normalised REE patterns of different facies from the Luni alluvium are presented in figure 5.4A and 5.4B. From the figures following observations can be made:

- The overall REE patterns are similar for all the facies, however, contents vary and so does the Eu anomalies.
- The Luni sediments show enriched LREE and flat HREE patterns, akin to upper continental rocks. This is expected as the catchment of the river is dominated with Precambrian crustal rocks.

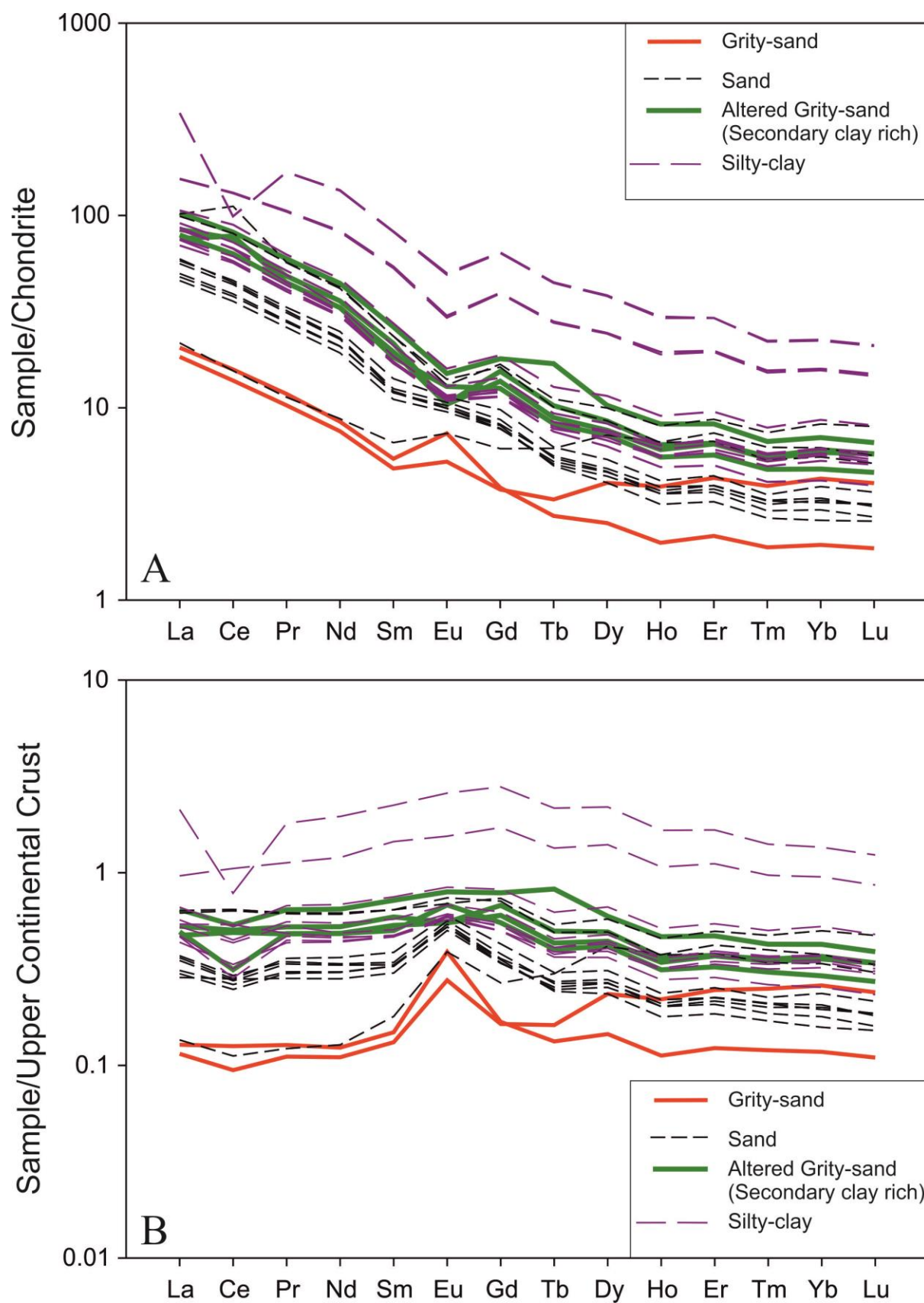


Figure 5.4: (A) Chondrite normalised and (B) Upper continental crust normalised REE patterns of different sedimentary facies observed in the Luni alluvium.

- Both the modern gritty-sand bedload sediments and the older gritty horizon (Pliocene) have lowest REE abundance and show positive Eu anomaly.
- The altered gritty horizons with clay matrix, however, shows negative Eu anomaly.
- The sand dominated facies has higher REE abundance than the gritty layers. They show no Eu anomaly or relatively small negative Eu anomaly.
- Silt and clay dominated finer sediments have highest abundance of REE and possess negative Eu anomaly.
- In the PAAS normalised REE patterns, the positive Eu anomalies become more pronounced. The gritty-sand layers have the most pronounced anomaly followed by the sandy horizons. The silt-clay rich layers show a more flattened REE pattern with no Eu anomaly.

It is generally assumed that the REE patterns of the sediments reflect that of their sources. However, REE patterns observed in sediments are dependent on many factors of which the most important being the degree of weathering. In case when the weathering is incipient and degree of chemical weathering is less, then the REE patterns of sediments may not truly represent the source (Singh and Rajamani, 2001). In such scenarios care must be taken before interpreting the data.

In case of the Luni alluvium, there are distinct differences in REE patterns among different sediment facies in spite of the fact that, the sediment source remained same (the Aravalli range). The sediment source region in the Aravalli receives limited rainfall and that too only for a limited period during the SW monsoon. Therefore, the source region of the river undergoes lower chemical weathering compared to the physical processes. In such an environment the more weathering prone mafic-ultramafic (and their metamorphic counterparts) rocks would weather faster than the gneissic and granitoid rocks. This would likely produce a chemical bias in the sediments, produced by the weathering in the Aravallis and carried by the Luni, towards that of the constituent minerals of the mafic/ultramafic rocks.

Furthermore, sediment transport in the ephemeral rivers like the Luni is highly seasonal and depends on the stream intensity. This causes a strong grain size sorting along the course of the river. Also, heavy transmission loss occurs downstream of the Luni river (Sharma et al., 1984). These factors would affect the ultimate chemistry of the sediments and make them

chemically dissimilar with the source. Considering these, our interpretation for the observed REE patterns in various sedimentary facies of Luni are as follows.

- The positive Eu anomalies observed in the gritty sediments (Fig. 5.4A and 5.4B) are most likely due to the presence of un-weathered plagioclase feldspars. The easily weathering prone source rocks in the catchment (the mafic-ultramafic rocks, meta-pelites etc.) have plenty of plagioclase feldspar in them. However, due to low degree of chemical weathering other constituent minerals (mafic ones) move out of the system much quickly leaving behind the quartz-plagioclase grains in the gritty horizons.
- The low abundance of REE in the sediments (Fig. 5.4A and 5.4B) can be explained by the quartz dilution effect. Also fewer amounts of the coatings of REE rich secondary phases over coarser fraction of sediments can be the reason for less abundant REE (Singh and Rajamani, 2001).
- In the sand dominated sediments the positive Eu anomaly becomes less pronounced and in some cases even negative (Fig. 5.4B). Due to accumulation of more REE bearing secondary phases the feldspar effect decreases in the sandy layers.
- The inference is further confirmed by the negative Eu anomaly observed in the fine grained clastics (silty-clay deposits) and altered gritty horizons. Singh and Rajamani, (2001) has observed similar signatures in the Kaveri alluvium and suggested that, in case of fine grained clastics, REE rich secondary phases create coatings over the grains occur which mask the feldspar effect and increase the elemental abundance of REE.

From these observations we infer that the trace element compositions of the Luni sediments are not true representatives of their sources. The REE abundance and the patterns are mainly controlled by the weathering intensity and sorting in the Luni basin. To constrain the sediment provenance we made use of the Sr-Nd isotopic fingerprinting.

### 5.3.2 Sr-Nd isotopic fingerprinting

The Sr-Nd isotopic composition of various sedimentary facies observed at the Luni alluvium are compared with that of various probable source rocks in the  $\epsilon_{Nd}$  vs.  $^{87}Sr/^{86}Sr$  bivariate plot (Fig. 5.5). A three component mixing grid is also presented in the figure for

quantifying the differential sediment contributions. From the figure the following inferences can be drawn.

- The mafic-ultramafic suit of rocks exposed along the western flank of the Aravalli ranges which stand high just above the piedmont region of the Luni, show low  $^{87}\text{Sr}/^{86}\text{Sr}$  and high  $\epsilon_{\text{Nd}}$ .
- The pelitic schists and calc-silicate rocks of the Delhi Supergroup show low  $\epsilon_{\text{Nd}}$  and low  $^{87}\text{Sr}/^{86}\text{Sr}$ .
- On the other hand the quartzite and other rocks of the Delhi Supergroup exposed along the western flank of the Aravalli Range show high  $^{87}\text{Sr}/^{86}\text{Sr}$  and low  $\epsilon_{\text{Nd}}$ . The Erinpura granites have comparable Sr-Nd isotopic ratios.
- The pockets of the BGC rocks exposed along the western margin of the Aravalli as well as the Malani rhyolites have different Sr-Nd isotopic ratios and do not seem to contribute much to the Luni alluvium.

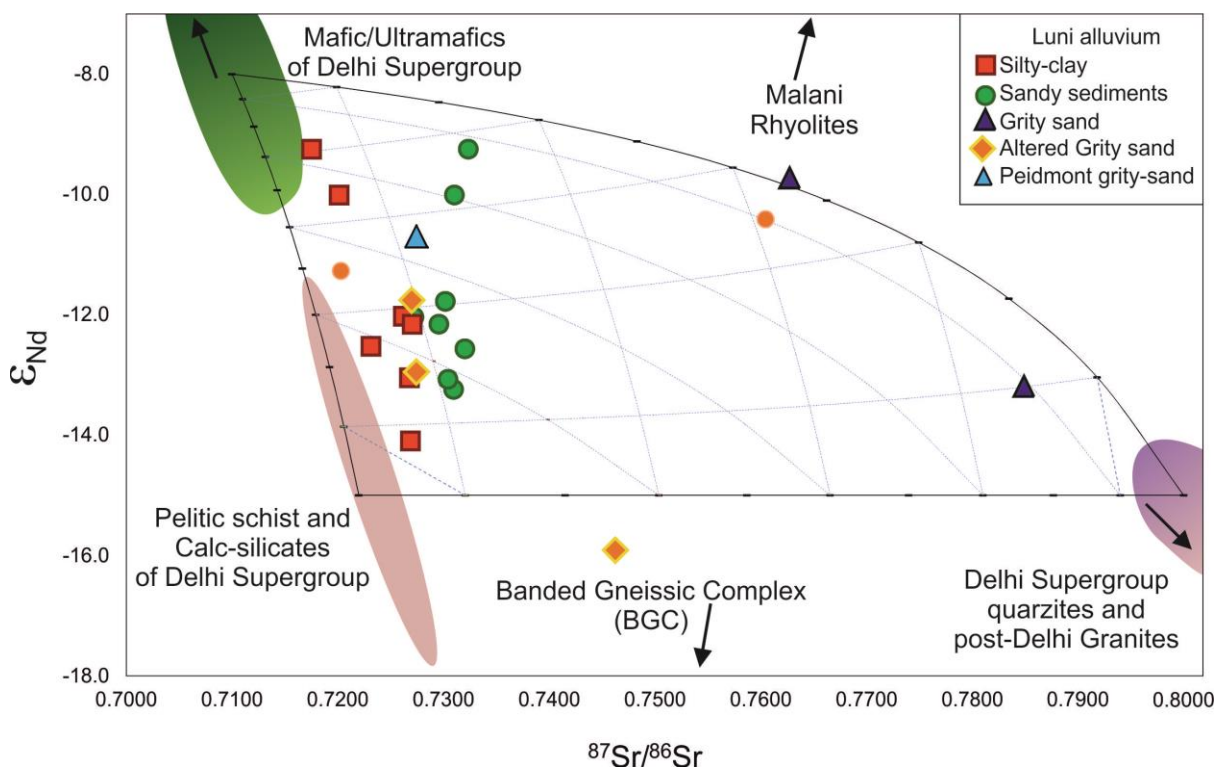


Figure 5.5:  $\epsilon_{\text{Nd}}$  vs.  $^{87}\text{Sr}/^{86}\text{Sr}$  plot of the Luni river sediments compared with a ternary mixing grid involving the probable sources. Data source for end-members: (George and Ray, 2017; Volpe and Macdougall, 1990).

- The contribution of the mafic-ultramafic suit of rocks and the schistose rocks of the Delhi Supergroup to the Luni river sediments can be easily discerned.
- Other important sediment contributors to the Luni alluvium are the metamorphosed rocks (pelitic schists and calc-silicates) of the Delhi Supergroup exposed along the western Aravalli Ranges.
- Other varieties of the Delhi Supergroup rocks such as the quartzite and the post-Delhi Erinpura Granite contribute very little to the Luni alluvium (~10%).

## 5.4 Conclusions

From our limited geochemical study of the Luni alluvium we concluded following about the sources of sediments deposited in this sink.

- The REE geochemistry of the Luni river sediments are mainly controlled by the weathering and sediment transport processes.
- Due to incipient weathering different sediment loads represent different REE patterns and abundances.
- The gritty-sand horizons show positive Eu anomalies due to the presence of unweathered plagioclase grains. However, the finer sediments have no such anomalies.
- Our study indicates that the REE patterns of the sediments generated in physical weathering dominated regions are influenced by the weathering and transportation processes rather than REE character of the source regions.
- The provenances have been identified by the Sr-Nd isotopic fingerprinting of the sediments. Major sediment sources of the Luni river alluvium are the mafic/ultramafic rocks, pelitic schists and calc-silicate rocks of the Delhi Supergroup. The post-Delhi granites and granitoids have contributed a little to the sediment budget of the basin.

Table 5.1 Trace element concentration and Sr-Nd isotopic composition of the Luni river sediments.

Samples	LUNI-2013-1 (Grit)	LUNI-2013-2	LUNI-2013-3(Silty clay)	LUNI-2013-4	LUNI-2013-5(Silty clay)	LUNI-2013-6(Silty clay)
Sc	0.53	3.57	7.7	4.35	11.53	6.53
V	5.67	29.2	55.34	30.1	138.2	122.4
Cr	100.9	205.3	78.67	82.44	85.19	91.94
Co	0.92	4.15	8.5	2.68	4.46	32.23
Cs	2.31	3.86	5.75	1.3	5.79	3.53
Rb	102.9	81.7	92.1	56	71	47.5
Ba	381	303	299	289	293	1328
Th	2.6	8.6	10.1	7	13.3	7.7
U	0.32	1.2	1.77	1.03	1.37	1.94
Nb	1	7	10	5	12	7
Ta	0.1	0.58	0.78	0.48	0.79	0.45
La	5	18	25	24	37	81
Ce	10	48	55	50	80	60
Pb	7.8	6.3	5.9	4.9	4.6	13.5
Pr	1.1	4.2	5.9	5.6	9.9	15.9
Sr	46	59	136	135	65	108
Nd	4	13	17	18	40	64
Zr	18	40	36	14	73	40
Hf	0.5	1.2	1.3	0.5	1.9	1.1
Sm	0.8	3	4.2	3.7	8.1	12.5
Eu	0.4	0.6	0.9	0.8	1.7	2.8
Gd	0.8	2.8	3.9	3.3	8.1	13.1
Tb	0.1	0.33	0.48	0.4	1.03	1.66
Dy	0.6	1.9	2.9	2.4	6.1	9.7
Y	3.1	7.3	10.1	10	31.6	47.8
Ho	0.11	0.34	0.51	0.43	1.07	1.66
Er	0.4	1.1	1.6	1.3	3.2	4.8
Tm	0	0.1	0.2	0.2	0.4	0.6
Yb	0.3	1	1.5	1.2	2.7	3.8
Lu	0.05	0.15	0.21	0.17	0.37	0.53
$^{87}\text{Sr}/^{86}\text{Sr}$	0.784908		0.723135		0.720122	0.717509
$\epsilon_{\text{Nd}}$	-13.2		-12.5		-10	-9.3
Samples	LUNI-2013-7 (Altered Grit)	LUNI-2013-8 (Sand)	LUNI-2013-9 (Altered Grit)	LUNI-2013-10 (Altered Grit)	LUNI-2013-11 (Grit)	KU-AEOLIAN
Sc	3.76	5.16	2.84	5.5	1.66	4.97
V	26.47	36.01	20.97	34.06	4.6	25
Cr	153.3	192.8	114.9	47.22	37.09	18.48
Co	2.85	4.05	2.04	3.36	0.7	1.86
Cs	3.76	2.37	1.41	1.67	1.49	1.78

Rb	76.6	71.6	45.5	56.6	63.8	64.6
Ba	281	343	219	271	246	336
Th	10.6	7.5	5.8	7.8	1.9	4.2
U	1.35	0.98	0.8	1.52	0.3	0.58
Nb	6	7	4	5	1	4
Ta	0.48	0.51	0.32	0.49	0.16	0.46
La	20	23	19	24	4	19
Ce	46	49	39	50	8	35
Pb	5.2	5.5	5.2	4.9	4.3	5.5
Pr	4.6	5.4	4.2	5.6	1	3.7
Sr	61	166	112	143	42	158
Nd	15	20	10	18	3	13
Zr	32	17	10	20	6	12
Hf	1.1	0.5	0.4	0.6	0.2	0.3
Sm	3.3	3.6	2.8	4	0.7	2.1
Eu	0.6	0.8	0.7	0.9	0.3	0.6
Gd	3.2	3.3	2.6	3.7	0.8	2
Tb	0.38	0.38	0.31	0.63	0.12	0.23
Dy	2.2	2.2	1.8	2.6	1	1.4
Y	8.2	10	5.4	10.3	5.3	6.4
Ho	0.36	0.37	0.31	0.47	0.22	0.25
Er	1.1	1.1	0.9	1.4	0.7	0.8
Tm	0.1	0.1	0.1	0.2	0.1	0.1
Yb	1	0.9	0.8	1.2	0.7	0.7
Lu	0.15	0.13	0.12	0.17	0.1	0.09
$^{87}\text{Sr}/^{86}\text{Sr}$	0.746266	0.727213	0.727464	0.727026	0.762735	
$\epsilon_{\text{Nd}}$	-15.9	-12	-13	-11.8	-9.7	
Samples	KU-1-CS (Silty clay)	KU-1-S (Sand)	KU-2-CS(Silty clay)	KU-2-S (Sand)	KU-3- CS(Silty clay)	KU-3-S (Sand)
Sc	3.72	2.96	7.98	3.47	6.47	3.48
V	29.82	20.57	60.95	21.82	56.15	24.03
Cr	20.73	13.94	43.86	15.65	37.85	16.36
Co	2.24	1.59	4.68	1.69	4.35	1.86
Cs	3.24	1.85	6.57	1.63	5.01	2.4
Rb	61.5	62.1	94.5	58.2	76.5	69.5
Ba	229	298	306	288	278	325
Th	6	4.4	7.1	3.7	5.9	4
U	0.95	0.54	1.34	0.56	1.16	0.75
Nb	5	3	9	3	8	4
Ta	0.39	0.26	0.68	0.35	0.72	0.38
La	18	13	20	11	17	12
Ce	35	27	41	23	35	24
Pb	4.7	5.5	4.2	5.2	4.2	5.3
Pr	3.9	3	4.7	2.6	3.8	2.7
Sr	106	141	122	141	102	137

Nd	9	9	13	8	11	9
Zr	12	7	38	10	31	16
Hf	0.6	0.3	1.3	0.3	1	0.5
Sm	2.6	1.9	2.8	1.8	2.6	1.8
Eu	0.6	0.6	0.7	0.6	0.6	0.6
Gd	2.3	1.7	2.6	1.7	2.3	1.6
Tb	0.28	0.19	0.31	0.21	0.3	0.19
Dy	1.6	1	1.9	1.2	1.7	1.1
Y	4.7	3.8	7.9	4.9	6.7	4.8
Ho	0.28	0.18	0.34	0.22	0.31	0.2
Er	0.8	0.5	1.1	0.6	1	0.6
Tm	0.1	0.1	0.1	0.1	0.1	0.1
Yb	0.7	0.4	1	0.5	0.9	0.6
Lu	0.1	0.07	0.14	0.08	0.13	0.08
$^{87}\text{Sr}/^{86}\text{Sr}$	0.726857	0.729562	0.726209	0.730178	0.726779	0.730967
$\epsilon_{\text{Nd}}$	-14.1	-12.2	-12	-11.8	-13	-13.2
Samples	KU-4- CS(Silty clay)	KU-4-S (Sand)	KU-5-CS(Silty clay)	KU-5-S (Sand)	KU-6- CS(Silty clay)	KU-6-S (Sand)
Sc	6.97	3.54	5.71	3.04	9.31	4.08
V	52.57	25.76	44.83	21.38	59.56	21.46
Cr	35.04	16.45	31.61	14.35	44.95	13.49
Co	3.88	1.94	3.35	1.6	4.44	1.56
Cs	5.17	2.54	4.27	1.98	6.26	2.24
Rb	84.6	65	69.1	62.7	105.5	76.6
Ba	291	294	237	302	368	340
Th	6.7	4.8	6.7	4.3	6.9	3.2
U	1.28	0.75	1.28	0.63	1.3	0.59
Nb	8	4	7	3	10	3
Ta	0.63	0.37	0.5	0.35	0.8	0.25
La	22	14	18	14	21	11
Ce	44	28	37	27	41	22
Pb	4.4	5.3	4.5	5.3	4.8	5.7
Pr	4.9	3.2	4.1	3	4.3	2.5
Sr	122	128	88	137	139	165
Nd	14	9	10	9	16	9
Zr	30	16	29	11	44	12
Hf	1	0.5	1.2	0.3	1.2	0.3
Sm	3.2	2.2	2.7	1.9	2.6	1.7
Eu	0.7	0.7	0.6	0.6	0.7	0.6
Gd	2.9	2	2.5	1.8	2.5	1.6
Tb	0.35	0.23	0.29	0.2	0.31	0.2
Dy	2.1	1.4	1.8	1.2	1.9	1.2
Y	7.7	5	6.3	4.7	10.4	6
Ho	0.36	0.24	0.32	0.2	0.36	0.21
Er	1.1	0.7	1	0.6	1.1	0.7

Tm	0.1	0.1	0.1	0.1	0.1	0.1
Yb	1	0.7	1	0.5	1	0.6
Lu	0.14	0.09	0.13	0.07	0.15	0.08
$^{87}\text{Sr}/^{86}\text{Sr}$	0.727042	0.730431		0.731032		0.732354
$\epsilon_{\text{Nd}}$	-12.2	-13.1		-10		-9.3
Samples	KU-7 (Sand)	KU-8 (Sand)	PH-15-13 (Piedmont sediment)			
Sc	1.1	9.3				
V	6.96	71.09				
Cr	3.86	50.34				
Co	0.78	7.31				
Cs	1.99	9.52				
Rb	96.4	124.6				
Ba	350	311				
Th	1.7	11.4				
U	0.42	1.67				
Nb	3	11				
Ta	0.3	0.83				
La	5	24				
Ce	10	68				
Pb	6.4	5.2				
Pr	1.1	5.4				
Sr	66	90				
Nd	4	15				
Zr	67	46				
Hf	1.7	1.7				
Sm	1	3.6				
Eu	0.4	0.8				
Gd	1.3	3.5				
Tb	0.23	0.41				
Dy	1.8	2.5				
Y	10.1	9.2				
Ho	0.37	0.45				
Er	1.2	1.4				
Tm	0.2	0.2				
Yb	1.1	1.4				
Lu	0.14	0.2				
$^{87}\text{Sr}/^{86}\text{Sr}$		0.732031	0.727464			
$\epsilon_{\text{Nd}}$		-12.6	-10.7			